These are the Supplementary Information for:

Lugli F., Cipriani A., Capecchi G., Ricci S., Boschin F., Boscato P., Iacumin P., Badino F., Mannino M.A., Talamo S., Richards M.P., Benazzi S., Ronchitelli A., *Strontium and stable isotope evidence of human mobility strategies across the Last Glacial Maximum in southern Italy*, Nature Ecology & Evolution (2019)

The final published version is available online at:

https://doi.org/10.1038/s41559-019-0900-8

https://www.nature.com/articles/s41559-019-0900-8

Supplementary Information for:

Strontium and stable isotope evidence of human mobility strategies across the Last Glacial Maximum in southern Italy

Federico Lugli[1,2], Anna Cipriani[2,3], Giulia Capecchi[4], Stefano Ricci[4], Francesco Boschin[4], Paolo Boscato[4], Paola Iacumin[5], Federica Badino[1,6] Marcello A. Mannino[7,8], Sahra Talamo[8], Michael P. Richards[8,9], Stefano Benazzi[1,8], Annamaria Ronchitelli[4]

[1]Department of Cultural Heritage, University of Bologna, Via degli Ariani 1, 48121 – Ravenna, Italy

[2]Department of Chemical and Geological Sciences, University of Modena and Reggio Emilia, Italy

[3]Lamont-Doherty Earth Observatory, Columbia University, Palisades, New York, USA

[4]Dipartimento di Scienze Fisiche, della Terra e dell'Ambiente, Unità di Ricerca Preistoria e Antropologia, Università degli Studi di Siena, Italy

[5]Department of Chemistry, Life Sciences and Environmental Sustainability, University of Parma, Parma, Italy

[6]C.N.R. – Istituto per la Dinamica dei Processi Ambientali, Laboratory of Palynology and Palaeoecology, Milan, Italy

[7]Department of Archaeology and Heritage Studies, School of Culture and Society, Aarhus University, Højbjerg, Denmark

[8]Department of Human Evolution, Max Planck Institute for Evolutionary Anthropology, Leipzig, Germany

[9]Department of Archaeology, Simon Fraser University, Burnaby, Canada

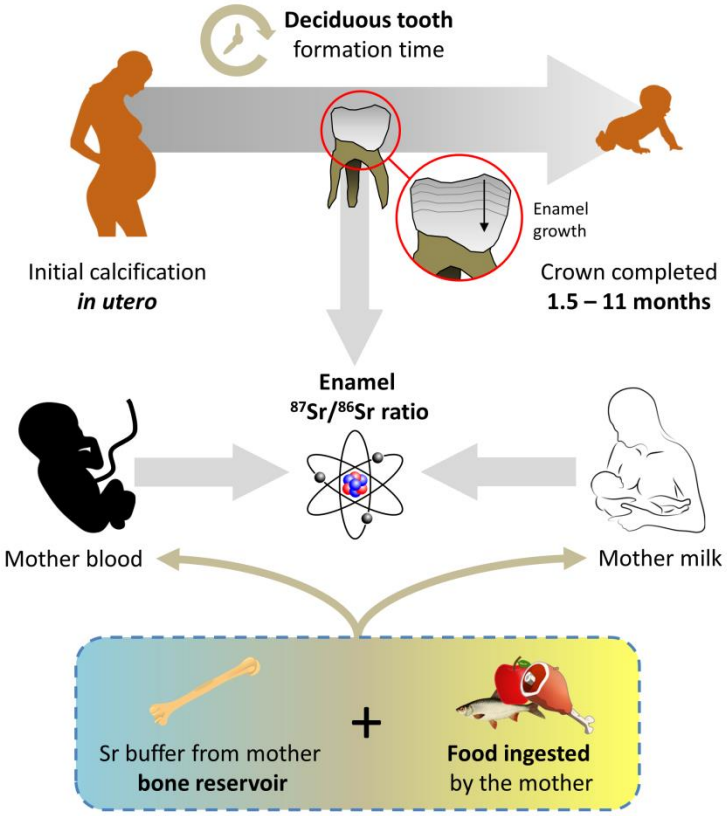

Figure S1. Descriptive model of Sr isotopes and deciduous tooth formation. From the initial intra-uterine calcification to the completion of the crown within the first year of life, enamel should register information about dietary habits of the mother of the individual. It is still not clear with which proportion the bone Sr reservoir contributes to the final $^{87}Sr/^{86}Sr$ ratio of the deciduous tooth.

Sr isotopes by LA-MC-ICP-MS

The enamel tissue of fourteen human deciduous teeth (six incisors, two canines and six molars, see Table 2) from Grotta Paglicci was micro-sampled by linear profiles (~750 x 100 µm) parallel to the tooth growth, following the cervix-apex direction. The number of laser scans per tooth varies between two and seven in relation to the tooth shape and presence of defects on the enamel surface. We avoided laser defocusing, firing only the flattest portion of the tooth specimen and tilting the tooth if focusing was not attainable (Balter et al., 2012). We employed a laser frequency of 10 Hz, a scan speed of 5 µm/s and a laser output of 100%, with a resulting fluence of ~17 J/cm^2. Dentine was also analyzed in a few teeth using the same analytical parameters. The following masses were acquired ^{88}Sr, ^{87}Sr, 86.5, ^{86}Sr, ^{85}Rb, 85.5, ^{84}Sr, ^{83}Kr, ^{82}Kr, using 10^{11} Ω amplifiers, with the exception of *m/z* 86.5 and 85.5 where 10^{12} Ω amplifiers were employed. Kr and Rb were measured to correct for interferences on Sr masses. Half-masses were used to check the formation of doubly-charged REE and to monitor the presence of diagenetic contaminant within the specimens. Enamel ^{88}Sr signals vary

between 0.5 and 1.5 V. Based on our protocol, all the analyses with ^{88}Sr signals < 0.5 V are inaccurate and thus discarded. During the analytical session, we also monitor the precision of the measures using a set of in-house tooth reference materials (Lugli et al., 2017b), whose Sr isotope ratios have been previously determined by solution MC–ICP–MS. These reference materials were also used to correct for the interference of $^{40}Ca^{13}P^{16}O$ and $^{40}Ar^{13}P^{16}O$ molecules on *m/z* 87 by daily calibration curves (Lugli et al., 2017b). The ST2 standard (shark tooth) gave a LA $^{87}Sr/^{86}Sr$ ratio of 0.70912 ± 0.00006 (2σ; n = 23) and an average laser ablation-solution difference ($\Delta_{LA\text{-}SOL}$) of -64 ppm. The BOS standard (bovine tooth) yielded a LA $^{87}Sr/^{86}Sr$ ratio of 0.70885 ± 0.00017 (2σ; n = 18) and a $\Delta_{LA\text{-}SOL}$ of 78 ppm. The SUS standard (swine tooth) a LA $^{87}Sr/^{86}Sr$ ratio of 0.70896 ± 0.00020 (2σ; n = 10) and $\Delta_{LA\text{-}SOL}$ of -31 ppm. These results are in agreement with previous analytical sessions by Lugli et al. (2017a, 2017b). Some of the human specimens (especially those from Gravettian layers) display intra-tooth variations higher than the 2σ of the swine tooth. These variations are not correlated with the number of analyses per sample (r^2 = 0.04) or with the tooth average ^{88}Sr signal (r^2 = 0.04), suggesting that they arise from natural factors rather than analytical uncertainties or sampling bias. A Pleistocene fossilized rhinoceros tooth was also analyzed together with our samples to assess the diagenetic condition of our human samples (see Diagenesis section).

Sr isotopes by solution MC-ICP-MS

Rodent (n = 16) and macro-mammal (n = 69) teeth were selected from the layers of Grotta Paglicci, according to the chronological distribution of human samples. Modern plants were sampled in the area surrounding Grotta Paglicci and each specimen is a pool of different arboreal plants, grown in natural areas away from roads and cultivated fields. Before Sr extraction, plant samples were ashed at 500° C for 6 hours. 1 to 10 mg of enamel and 5 mg of plant ashes were leached, digested and Sr was separated following procedures detailed in Lugli et al. (2017a). Sr isotope ratios were measured by MC–ICP–MS on a Neptune mass spectrometer housed at the CIGS (UNIMORE). Data were corrected through exponential law to a $^{88}Sr/^{86}Sr$ ratio of 8.375209. During this analytical session, the standard yielded a $^{87}Sr/^{86}Sr$ ratio of 0.710239 ± 0.000014 (2σ; n = 28). The Sr ratios were reported to a NBS–987 value of 0.710248 (McArthur et al., 2001). Total Sr blanks did not exceed 100 pg.

The local baseline of Grotta Paglicci

Modern plants sampled from the surroundings of the Grotta Paglicci site were analyzed to build a local *isoscape* as baseline for isotopic variations of the bioavailable Sr (Fig. 1 and Table 1, main text). Their $^{87}Sr/^{86}Sr$ ratios range between 0.70813 and 0.70898 (mean: 0.70846 ± 0.00043; *n* = 27) in agreement with the local bedrock geology, mostly composed of carbonate rocks ranging from the Middle Jurassic to the Miocene (Pellegrini et al., 2008). Recent alluvial deposits are present around the site and range in age from the Pleistocene to the Holocene (Tafuri et al., 2016).

Rodent teeth (dentine plus enamel) collected from the Gravettian and Epigravettian layers of the site have an average $^{87}Sr/^{86}Sr$ ratio of 0.70842 ± 0.00016 (*n* = 16). Given that rodents generally present a limited home-range size (~1-5 km; Clapperton, 2006), their isotopic composition should reflect a mix of the local bioavailable Sr and the local diagenetic Sr. We did not identify any specific time-related trend in the $^{87}Sr/^{86}Sr$ ratios of these teeth, as expected for local specimens slightly homogenized by the local diagenetic imprint. Moreover, the rodent teeth Sr isotope composition is statistically indistinguishable from that one of modern plants (two-tailed Mann-Whitney U-test; *p* = 0.42952). Considering all the local proxies, an interval between 0.7080 and 0.7088 can be conservatively considered as the broadest and most likely local Sr isotope composition range of Grotta Paglicci.

Macro-mammals (*Capra ibex*, *Equus ferus* and *Equus hydruntinus*), sampled from the same layers of the human teeth, were also analyzed to compare their mobility pattern with those of humans (Fig. 2, main text). The macro-mammals Sr isotope ratios, obtained through total dissolution of the specimen, range from 0.70813 to 0.70881 (mean: 0.70856 ± 0.00023, *n* = 69). In particular, *Capra ibex* specimens show an average $^{87}Sr/^{86}Sr$ ratio of 0.70856 ± 0.00014; *Equus ferus* an average $^{87}Sr/^{86}Sr$ ratio of 0.70854 ± 0.00028; while *Equus hydruntinus* an average $^{87}Sr/^{86}Sr$ ratio of 0.70861 ± 0.00025. Macro-mammals exhibit the lowest $^{87}Sr/^{86}Sr$ ratios during the Early Gravettian (~0.7081), in particular for *Equus ferus* (Table 1, main text).

Human dentine was also analyzed *in situ* in three human tooth specimens. Sample PA129 (Early Gravettian) yielded a dentine $^{87}Sr/^{86}Sr$ ratio of 0.70816 ± 0.00008 (2se), sample PA95 (Evolved Gravettian) a ratio of 0.70859 ± 0.00004 (2se), while sample PA83 (Epigravettian) a ratio of 0.70884 ± 0.00008 (2se). Being dentine tissue highly susceptible to diagenetic contamination, its $^{87}Sr/^{86}Sr$ ratio should reflect linear mixing between the biogenic signal and the diagenetic Sr (see Fig. S2 and S3). The dentine specimens present isotopic values that reflect the increasing temporal trend of the enamel $^{87}Sr/^{86}Sr$ ratios, but shifted above the local isotope baseline possibly due to diagenetic processes (Fig. 2, main text).

Sr isotopes of a deciduous tooth

Although deciduous teeth are used for Sr isotope studies, it is not clear yet whether they retain or not time-resolved isotopic information or the timing that this information is recorded within the tooth enamel. Some have suggested that the different waves of mineralization, occurring during amelogenesis, may average the isotopic ratio obtained from the outer enamel surface (OES) analysis (e.g. Montgomery et al., 2010). Others have questioned whether the bone Sr reservoir of the mother may contribute to the final isotope ratio (Lugli et al., 2017a). Nevertheless, isotope analyses of permanent teeth in high-spatial resolution suggest that mineralization only partially affects the isotope ratio of the OES, which, in turns, still retains reliable chronological isotopic information (e.g. Lugli et al., 2017b).

Diagenesis

Enamel is almost completely mineralized and is the strongest tissue of a tooth. Consequently, its structure and composition are usually not altered by diagenetic processes (Budd et al., 2000). In fact, many chemical/isotopic studies of old/fossil teeth have relied solely on enamel to retrieve reliable biogenic information (e.g. Lee-Thorp and Sponheimer, 2003; Wright, 2005; Bentley, 2006; Evans et al., 2006; Copeland et al., 2008; Pellegrini et al., 2008; Richards et al., 2008; Copeland et al., 2011; Slovak and Paytan, 2011; Balter et al., 2012; Willmes et al., 2016). However, several reports have also indicated how enamel over long periods can be altered, especially in extreme environments (e.g. Michel et al., 1995; Sponheimer et al., 2006; Jacques et al., 2008). Unlike enamel, bone and dentine tissues are composed by a higher portion of organic matter (mainly collagen). Moreover, their physical structure is more porous, allowing the permeation of diagenetic fluids (Lee-Thorp and Sponheimer, 2003; Tütken et al., 2011). In particular, fresh bone is composed by nm-size crystals (~50 x 25 x 2-4 nm; Berna et al., 2004) of carbonate hydroxyapatite (~70%), organic matter (~20%) and water (~10%). During bone fossilization, collagen hydrolyzes, leaving apatite crystals exposed to ground fluids. The crystal lattice defects combined with a large surface area make the apatite highly susceptible to mineral dissolution-reprecipitation processes (Trueman and Tuross, 2002; Herwartz et al., 2013). The spaces left empty by the collagen are thus occupied by authigenic apatite. Consequently, trace elements of the diagenetic fluids can be incorporated within the apatite crystal lattice during recrystallization, while most of the trace elements are only adsorbed by surface sites (Herwartz et al., 2013).

In this work, we checked the diagenetic status of our human teeth using Rare Earth Element (REE) content as a proxy for post-depositional alterations. In fact, fossil teeth tend to present overly high REE concentrations (Trueman and Tuross, 2002) in comparison with modern bioapatites due to diagenetic uptake. We monitored any potential REE enrichment on *m/z* 82 ($^{164}Er^{2+}$ + $^{164}Dy^{2+}$ + Ca dimers and argides) and 86.5 ($^{173}Yb^{2+}$), using 10^{12} Ω resistors. During the LA-MC-ICP-MS analytical session, we examined a Pleistocene (c.a. 600 kyrs old) fossil tooth enamel (MP-fossil), known to be partially diagenized. LA-ICP-MS analyses of this tooth revealed REE variations from <1 ppm to hundreds of ppm. In particular, Dy ranges between 2 and 137 ppm, while Yb from 0.8 to 63 ppm. Concerning the LA-MC-ICP-MS analysis, the MP-fossil shows a 82 *m/z* signal ranging from $2.4*10^{-3}$ to $1.6*10^{-4}$ V and a 86.5 *m/z* signal ranging from $1.9*10^{-4}$ to $7.4*10^{-6}$ V. Averagely, human enamel has values far lower than the MP-fossil signals (82 *m/z* = $3.7*10^{-5} \pm 9.3*10^{-5}$ V; 86.5 *m/z* = $3.8*10^{-6} \pm 6.6*10^{-6}$ V; 1σ; negative values excluded), and occasionally lower than the background itself. As expected, human dentine has slightly higher REE values (82 *m/z* = $3.6*10^{-4} \pm 3.5*10^{-4}$ V; 86.5 *m/z* = $6.2*10^{-6} \pm 3.6*10^{-6}$ V; 1σ). Results are summarized in Figure S2 and Figure S3. Overall, these results indicate that human tooth enamel does not present a high degree of diagenetic alteration, suggesting that the retrieved isotopic signals can be considered as biogenic. Contrariwise, dentine with higher REE content than human enamel could be considered as slightly diagenetically altered.

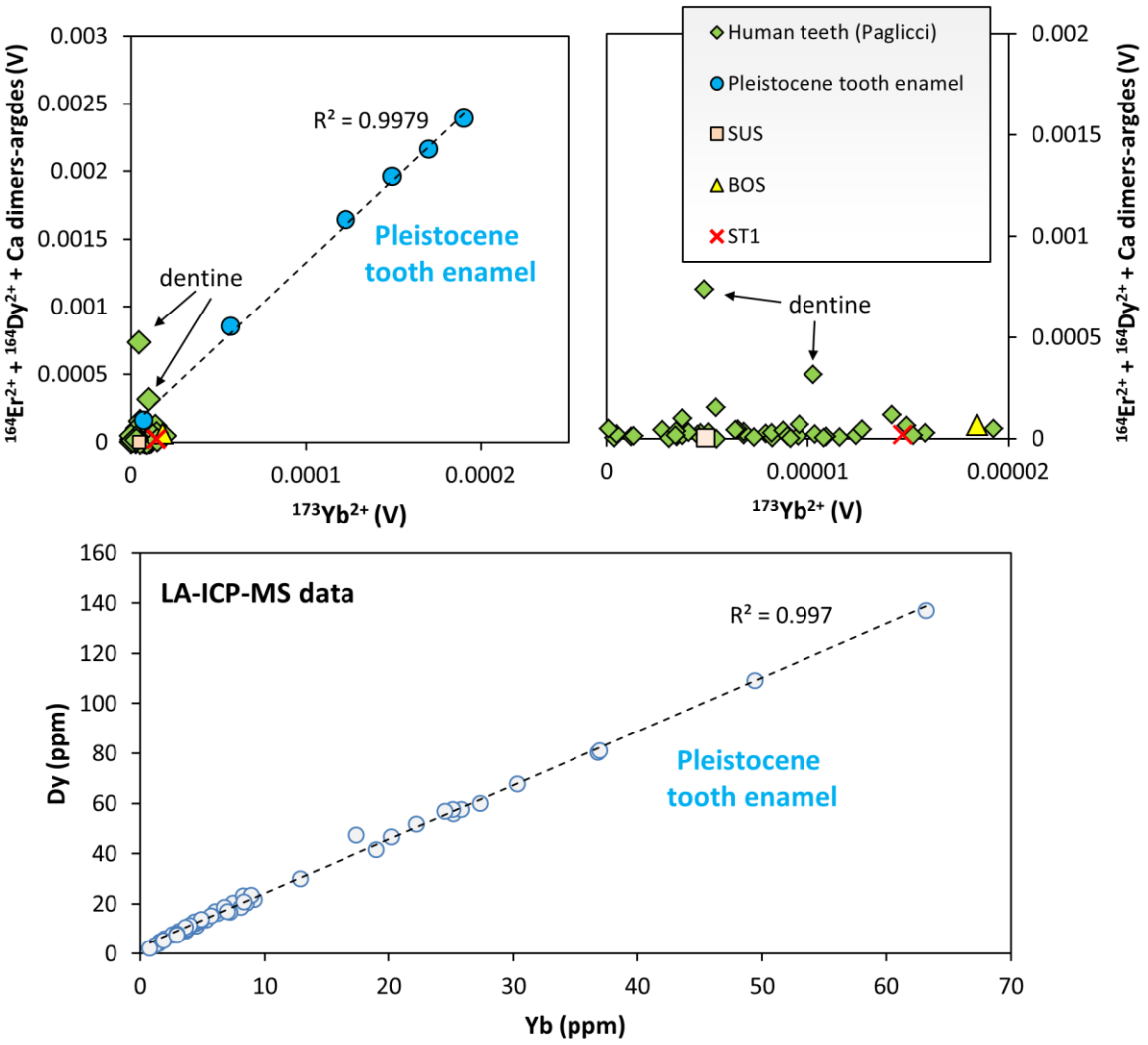

Figure S2. Diagenetic screening of the human teeth. Masses 82 ($^{164}Er^{2+}$ + $^{164}Dy^{2+}$ + Ca dimers and argides) and 86.5 ($^{173}Yb^{2+}$) were monitored during the LA-MC-ICP-MS analysis and compared with a known Pleistocene fossil tooth. Modern and archaeological teeth (ST2, SUS and BOS) are also reported for comparison. LA-ICP-MS data of the Pleistocene fossil tooth enamel (MP-fossil) reveal a great variability in terms of REE content.

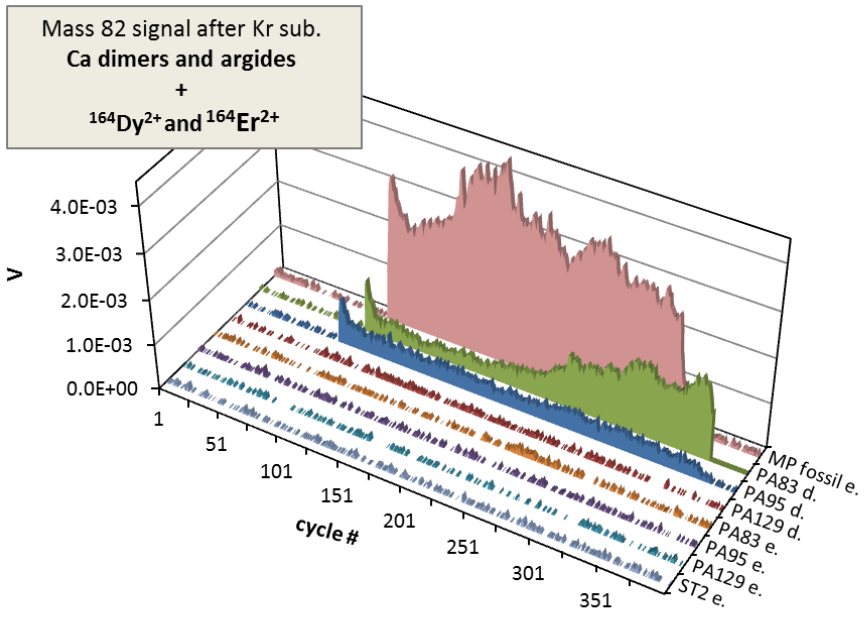

Figure S3. Examples of time-resolved *m/z* 82 signals for different specimens; "e." is for enamel, while "d." is for dentine.

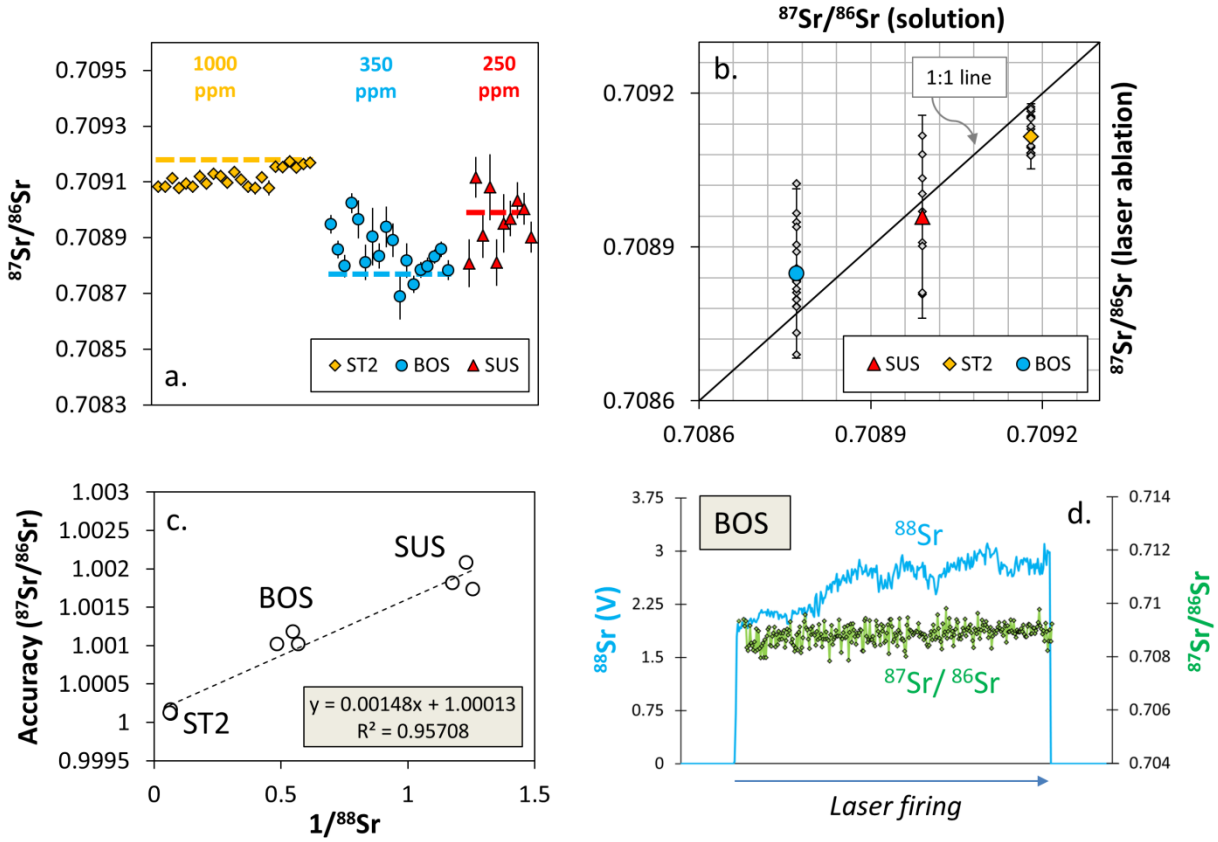

Figure S4. Summary of the Sr isotope data of reference materials (RMs) analyzed during this study; (a) the three RMs are grouped by their average Sr content (ppm) and compared with the solution MC-ICP-MS values (dashed line); (b) when laser ablation and solution results are compared, they plot on a 1:1 line, with higher errors observed for LA-MC-ICP-MS analyses; (c) example of a calibration curve employed for the correction of $^{40}Ca^{13}P^{16}O$ and $^{40}Ar^{13}P^{16}O$ interferences on *m/z* 87 ($R^2 > 0.9$; $p < 0.01$); (d) example of the resulting ^{88}Sr signal and the corrected $^{87}Sr/^{86}Sr$ ratio of a linear profile during BOS analysis.

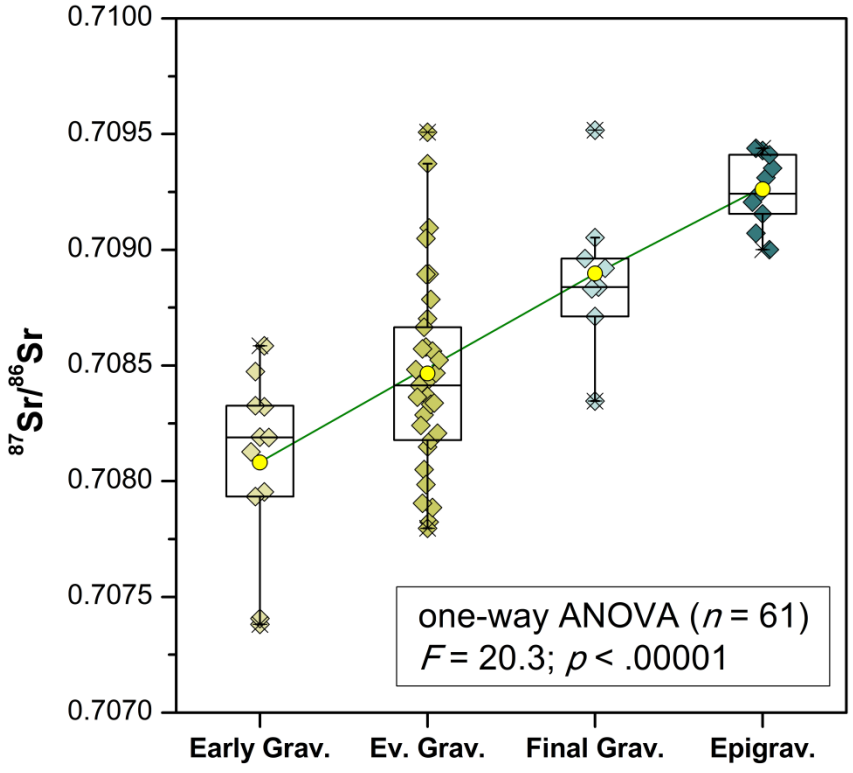

Figure S5. Human Sr isotope variability among different periods. Small squares are single LA data. Yellow circles are the average values for each period.

Figure S6. Human deciduous teeth from Grotta Paglicci.

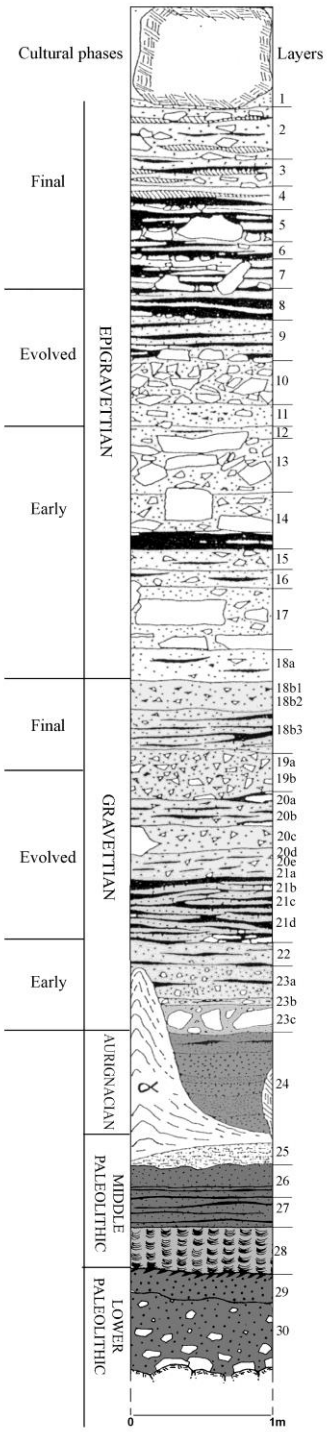

Figure S7. Stratigraphy of the Grotta Paglicci site (adapted from Ronchitelli et al., 2015).

Table S1. Radiocarbon dates from Grotta Paglicci (as reported in Berto et al., 2017).

Archaeological layer	Lithic industry	Lab ID#	Sample	^{14}C date	Cal BP 2σ (IntCal 13)
3a	Final Epigravettian	F-94		11440 ± 180	12970-13712
4	Final Epigravettian	F-95		11950 ± 190	13370-14429
5 bc	Final Epigravettian	F-96		13590 ± 200	15841-17021
6	Final Epigravettian	F-64		14270 ± 230	16696-17955
7	Final Epigravettian	F-65		14820 ± 210	17551-18541
7 c	Final Epigravettian	Ly-1628		13720 ± 870	14078-18867
8	Evolved Epigravettian	F-66		15460 ± 220	18220-19245
9	Evolved Epigravettian	F-67		15270 ± 220	18002-18956
10	Evolved Epigravettian	F-68		15320 ± 250	17988-19112
12 a	Early Epigravettian	GrN-14316	Charcoal	15950 ± 350	18549-20133
12 c	Early Epigravettian	GrN-14317	Charcoal	15730 ± 330	18334-19860
13 a	Early Epigravettian	GrN-14318	Charcoal	15480 ± 150	18405-19053
13 b	Early Epigravettian	GrN-14319	Charcoal	16310 ± 350	18892-20539
13 c	Early Epigravettian	GRN-14320	Charcoal	15990 ± 160	18901-19683
13 d	Early Epigravettian	GRN-14321	Charcoal	16030 ± 190	18896-19831
14 b (a)	Early Epigravettian	UtC-		15600 ± 200	18451-19384
14 b (b)	Early Epigravettian	GrN-14322	Charcoal	15930 ± 200	18786-19716
15	Early Epigravettian	UtC-		17100 ± 300	19929-21491
15 a	Early Epigravettian	GrN-14323	Charcoal	15570 ± 160	18499-19212
15 b	Early Epigravettian	GrN-14324	Charcoal	16260 ± 160	19211-20043
16	Early Epigravettian	UtC-		17200 ± 300	20040-21601
16 a3-1	Early Epigravettian	GrN-14325	Charcoal	16690 ± 150	19741-20531
16 b3 (a)	Early Epigravettian	GrN-14326	Charcoal	16450 ± 190	19396-20361
16 b3 (b)	Early Epigravettian	GrN-14870		16970 ± 150	20075-20861
16 b5	Early Epigravettian	GrN-14871		16750 ± 150	19828-20597
16 b7	Early Epigravettian	GrN-14872		16480 ± 150	19521-20272
16 c2	Early Epigravettian	GrN-14873		16850 ± 150	19952-20707
17 b	Early Epigravettian	GrN-14874		16890 ± 160	19979-20789
17 d1	Early Epigravettian	GrN-14875		17050 ± 160	20136-20989
17 e (a)	Early Epigravettian			19600 ± 300	22893-24322
17 e (b)	Early Epigravettian	GrN-14876		16940 ± 160	20029-20849
17 f	Early Epigravettian	GrN-14877		16790 ± 160	19855-20665
18 b2 (a)	Final Gravettian	F-44	Burnt bone	20200 ± 305	23612-25185
18 b2 (b)	Final Gravettian	R-1324		17200 ± 150	20355-21191
18 b2 (c)	Final Gravettian	F-43	Charcoal and charred bone	14260 ± 280	16529-18042
18 b3	Final Gravettian	F-45	Charcoal	20160 ± 310	23555-25157
19 a	Final Gravettian	F-46	Charcoal	20730 ± 290	24265-25660
20 b	Evolved Gravettian	F-47	Charcoal	21260 ± 340	24643-26184
20 c (a)	Evolved Gravettian	F-49	Burnt bone	22110 ± 330	25815-27174
20 c (b)	Evolved Gravettian	F-48	Charcoal	22220 ± 360	25870-27290
20 de	Evolved Gravettian	F-50	Charcoal	22630 ± 390	26114-27594
21 a	Evolved Gravettian	F-51	Charcoal	23040 ± 380	26468-27912
21 b	Evolved Gravettian	F-57	Charcoal	23470 ± 370	27070-28430
21 c (a)	Evolved Gravettian	F-53	Burnt bone	23750 ± 390	27326-28664
21 c (b)	Evolved Gravettian	F-54	Charcoal	24210 ± 410	27602-29128
21 d	Evolved Gravettian	F-55	Bone nr. 22	24720 ± 420	27871-29749
22 b	Early Gravettian	UtC-1412	Charcoal	26800 ± 300	30493-31330
22 f4	Early Gravettian	UtC-1413	Charcoal	28300 ± 400	31355-33329
23 a	Early Gravettian	UtC-1414	Charcoal	28100 ± 400	31210-33103
23 b	Early Gravettian	Utc-1415	Charred bone	26300 ± 400	29613-31121
24 a1	Aurignacian	UtC-1789	Charcoal	29300 ± 500	32112-34447
24 b1	Aurignacian	UtC-1790	Charcoal	34300 ± 900	36570-40939

Table S2. Strontium isotope composition and sampling location of the modern plant samples.

Sample ID #	$^{87}Sr/^{86}Sr$	2 SE	Coordinates
1	0.70876	0.00001	41°41'18.6"N 15°39'45.1"E
2	0.70837	0.00002	41°40'52.8"N 15°39'23.6"E
3	0.70828	0.00001	41°39'53.5"N 15°40'04.3"E
4	0.70817	0.00001	41°37'19.6"N 15°39'12.1"E
5	0.70825	0.00001	41°38'12.2"N 15°38'42.6"E
6	0.70813	0.00001	41°38'26.3"N 15°37'45.5"E
7	0.70836	0.00001	41°39'16.5"N 15°36'54.2"E
9	0.70851	0.00001	41°39'54.3"N 15°36'20.2"E
10	0.70868	0.00003	41°40'42.5"N 15°34'40.5"E
11	0.70822	0.00001	41°41'17.4"N 15°35'06.3"E
12	0.70849	0.00005	41°42'15.0"N 15°35'16.6"E
13	0.70846	0.00001	41°42'32.6"N 15°31'01.5"E
14	0.70843	0.00001	41°40'38.4"N 15°33'17.7"E
15	0.70833	0.00001	41°40'15.6"N 15°33'37.7"E
16	0.70861	0.00001	41°44'43.0"N 15°49'08.5"E
17	0.70865	0.00002	41°45'31.7"N 15°41'36.6"E
18	0.70850	0.00002	41°48'32.1"N 15°34'35.4"E
19	0.70898	0.00002	41°46'56.1"N 15°28'16.2"E
20a	0.70857	0.00001	41°39'09.9"N 15°29'26.8"E
20b	0.70854	0.00001	41°37'38.8"N 15°31'08.9"E
21	0.70858	0.00001	41°34'35.2"N 15°32'59.7"E
22	0.70853	0.00001	41°31'33.8"N 15°42'01.9"E
23	0.70816	0.00001	41°31'33.8"N 15°42'01.9"E
24	0.70841	0.00001	41°41'41.9"N 16°03'02.2"E
25a	0.70878	0.00001	41°47'59.4"N 15°59'06.4"E
25b	0.70866	0.00001	41°48'54.0"N 15°59'26.9"E
26	0.70815	0.00004	41°41'33.5"N 15°46'21.5"E

Table S3. Isotope and elemental composition of bone collagen from the Gravettian humans buried at Grotta Paglicci. '% coll.' is the abbreviation of percentage of the collagen extracted from the subsample of pretreated bone.

Lab. N. (S-EVA)	Context	Burial	Bone	$\delta^{13}C$ (‰)	$\delta^{15}N$ (‰)	%C	%N	C:N	% coll.
28202	layer 21 base	Paglicci 12	ulna?	-18.8	13.9	40.9	14.4	3.3	6.9
13777	layer 21	Paglicci 25	rib	-18.4	13.0	42.7	14.9	3.4	2.1

Carbon and nitrogen stable isotopes of bone collagen at the MPI

Bone pretreatment method used on the two Gravettian individuals (PA12 and PA25) is the one established by Talamo and Richards (2011) and was performed at the Max Planck Institute for Evolutionary Anthropology in Leipzig. The outer surface of the samples was first cleaned with a shot blaster and then a sub-sample of bone was taken. The samples were decalcified in 0.5M HCl at room temperature, until no effervescence was observed. 0.1M NaOH was added for 30 minutes to remove humics. The NaOH step was followed by a final 0.5M HCl step for 15 minutes. The resulting solid was gelatinized following Longin (1971) at pH3 in a heater block at 75°C for 20h. The gelatin was then filtered in an Eeze-Filter™ (Elkay Laboratory Products) to remove small (>80 μm) particles. The gelatin was then ultrafiltered with Sartorius "Vivaspin Turbo" 30 KDa ultrafilters (Brown et al. 1988). Prior to use, the filters were cleaned to remove carbon containing humectants (Brock et al. 2007). Samples were then lyophilized for 48 hours and extracts weighed to establish the percentage yield obtained from the subsampled bones. The isotope analyses were conducted at the Max Planck Institute for Evolutionary Anthropology in Leipzig on a Thermo Finnigan Delta V Advantage Isotope Ratio Mass Spectrometer (IRMS) coupled to a Flash 2000 EA. The analytical error is 0.2‰ (1σ). The ulna Paglicci 12 (S-EVA 28202) and the rib of Paglicci 25 (S-EVA 13777) have extracts compatible with well-preserved collagen according to the criteria proposed by van Klinken (1999), given that their elemental (%C, %N) and isotopic (δ^{13}, $\delta^{15}N$) compositions, C:N ratios and yields fall within accepted biogenic ranges (Table S3).

Carbon and nitrogen stable isotopes of bone collagen at the University of Parma

Bone collagen of the Epigravettian human specimens (PA85 and PA89) was extracted at the Stable Isotope Laboratory of the University of Parma, following the protocol described in Longin (1971) and modified by

Ambrose (1990) and Bocherens et al. (1991). The $\delta^{13}C$ and $\delta^{15}N$ were measured by means of a CHN elemental analyzer coupled with a mass spectrometer. The C:N ratios of the two samples fall within the 2.9–3.6 range for good collagen preservation (Van Klinken, 1999). The routinely 1σ uncertainties of the standards are ±0.2‰ for $\delta^{13}C$ and ±0.1‰ for $\delta^{15}N$.

Grotta Paglicci stable isotope baseline (from Iacumin et al., 1997)

The summary statistics for the three main macro-mammals species throughout the Paglicci sequence are as follows: *Cervus elaphus* ($\delta^{13}C$: range = -22.4‰ to -19.8‰, mean = -20.6 ± 0.7‰; $\delta^{15}N$: range = 5.0‰ to 8.5‰, mean = 6.5 ± 0.9‰), *Bos primigenius* ($\delta^{13}C$: range = -20.9‰ to -17.8‰, mean = -19.5 ± 0.7‰; $\delta^{15}N$: range = 6.1‰ to 11.9‰, mean = 7.9 ± 1.4‰) and *Equus ferus* ($\delta^{13}C$: range = -21.3‰ to -19.1‰, mean = -20.2 ± 0.6‰; $\delta^{15}N$: range = 4.3‰ to 8.4‰, mean = 6.8 ± 1.2‰).

Carbon and nitrogen isotope analyses: additional discussion

Taken together the inhumated Gravettian individuals (Paglicci 12 and Paglicci 25) have the highest $\delta^{15}N$ values of those recorded on humans belonging to the same culture (Richards et al. 2001; Bocherens et al. 2015). The $\delta^{13}C$ values are also high, suggesting that the occupants of Grotta Paglicci consumed more freshwater, marine and/or anadromous resources than other Gravettians with the exception of the so-called Prince from Arene Candide in Liguria (Pettitt et al. 2003) and the individual from La Rochette in France (Richards 2009). In the absence of a better trophic isotope baseline for Grotta Paglicci, it is hard to establish precisely which ecosystem other than the terrestrial one contributed the secondary, albeit relevant proportion of dietary protein attested for Paglicci 12 and Paglicci 25. Nevertheless, based on what is known for recent hunter-gatherers (e.g. Binford 1980, 2001; Kelly 2007), regular exploitation of freshwater, marine or mixed (anadromous/catadromous) resources is generally associated with higher logistical mobility and organizational costs, which may have been typical for Gravettian groups in the Italian peninsula.

The Epigravettian human specimens object of the carbon and nitrogen isotope analysis (PA85 from layer 10-14 and PA89 from layer 16b) post-date the Last Glacial Maximum, when there were frequent climatic oscillations from continental to Mediterranean conditions. The absence of direct dates on specimens PA85 and PA89 makes it difficult to establish whether these individuals endured colder/drier and/or milder/wetter conditions. The fact that despite the cold conditions present during the accumulation of layer 16 (Berto et al. 2017), the

Epigravettians from this phase had a different mobility pattern to the Gravettians, may be due to the fact that their subsistence and territoriality were different due to differences in culturally-driven strategies. The fact that the isotope composition of PA85 is similar to that of the Gravettian individuals may be due to the combined presence of more continental conditions and greater availability of aquatic habitats in the phase represented by layers 10-14 than at the time of the accumulation of layer 16b, although it should be noted that the environmental data are scarce for the time comprised between layers 14 and 11 (Berto et al. 2017).

A recent review of available isotopic data for the Upper Palaeolithic and Mesolithic of the central Mediterranean (Mannino and Richards 2018) has suggested that at times of climatic deterioration hunter-gatherers in this region consumed more aquatic foods, which may have been the case of the Epigravettian individual PA85. This does not necessarily imply that the Epigravettian groups in question had adopted logistical mobility strategies, but it can be explained by the regular or more frequent positioning of home bases in proximity to marine or freshwater habitats, which granted access to aquatic resources abundant at least during one season of the year. This possibility is also in line with the general increase in landscapes with rivers, lakes and ponds proposed for the area around Grotta Paglicci by the study of the small mammal skeletal assemblage (Berto et al. 2017).

Independently of the possible culturally-driven norms linked to territoriality that may have existed between Gravettian and Epigravettian groups, it should be pointed out that the environmental conditions under which they operated were slightly different and this may have influenced their mobility. In environments with more clumped resources (both spatially and temporally) higher return rates are possible by adopting complex mobility strategies in which camps are moved to specific locations in the landscape and result in lower overall mobility (Janssen and Hill, 2016), which was probably the case of the Gravettian occupants of Paglicci. On the other hand, the Epigravettians may have moved more frequently at least in part because they operated under more homogeneous environmental conditions (with the exception of cold phases in the Late Glacial), which not only led to increased mobility, but also possibly favoured a more random positioning of base camps.

Table S4. Enamel microsample Sr isotopes of Grotta Paglicci human deciduous teeth, obtained from each single LA track.

Technocomplex	Tooth specimen	Enamel $^{87}Sr/^{86}Sr$	2se
Epigravettian	PA82	0.70931	0.00015
		0.70943	0.00011
		0.70916	0.00014
	PA83	0.70924	0.00015
		0.70935	0.00017
		0.70944	0.00010
		0.70907	0.00010
	PA87	0.70921	0.00014
		0.70900	0.00011
		0.70941	0.00009
Final Gravettian	PA90	0.70884	0.00016
		0.70835	0.00020
	PA91	0.70871	0.00008
		0.70883	0.00008
		0.70905	0.00006
		0.70892	0.00007
		0.70896	0.00007
		0.70952	0.00006
Evolved Gravettian	PA92	0.70890	0.00015
		0.70815	0.00014
	PA93	0.70909	0.00016
		0.70844	0.00021
		0.70805	0.00012
		0.70837	0.00010
		0.70858	0.00009
		0.70782	0.00011
	PA94	0.70870	0.00015
		0.70866	0.00014
		0.70799	0.00015
		0.70829	0.00010
		0.70905	0.00007
		0.70951	0.00004
		0.70937	0.00005
	PA95	0.70889	0.00010
		0.70879	0.00011
		0.70833	0.00012
		0.70780	0.00010
	PA111	0.70856	0.00011
		0.70857	0.00008
		0.70847	0.00008
		0.70824	0.00012
		0.70841	0.00014
	PA112	0.70834	0.00013
		0.70789	0.00016
		0.70836	0.00015
		0.70790	0.00015
	PA40	0.70818	0.00014
		0.70821	0.00015
		0.70852	0.00015
		0.70848	0.00016
Early Gravettian	PA129	0.70832	0.00011
		0.70795	0.00009
		0.70833	0.00010
		0.70738	0.00012
	PA130	0.70859	0.00009
		0.70793	0.00013
		0.70819	0.00012
		0.70813	0.00011
		0.70819	0.00012
		0.70847	0.00009
		0.70741	0.00016

Table S5. Root resorption and age-at-death of human teeth from Grotta Paglicci considered in this study.

Technocomplex	Layer	Sample	Tooth element	Root resorption stage*	Age-at-death (yrs)
Early Epigravettian	12f	PA82	Ldi^2	Res ¾	> 8
	14	PA83	Ldi^2	Res ¾	> 8
	16a	PA87	Rdm^1	> Res ¾	> 11.5
Final Gravettian	18b	PA90	di(?)	Res ¾	> 8
	19a	PA91	Rdm^1	> Res ¾	> 11.5
Evolved Gravettian	20d	PA92	Rdm^1	n.d.	< 11
	20d	PA93	Rdm_1	n.d.	< 11
	20d	PA94	Ldm_1	n.d.	< 11
	20e	PA95	di^1	> Res ¾	> 7.5
	21c	PA111	Ldi^1	Rc-A ½	~ 2
	21c	PA112	Ldc_*	Rc-A ½	~ 2
	21d	PA40	Rdm_2	A ½	~ 3
Early Gravettian	22e	PA129	Ldc^*	> Res ¾	> 11
	23a	PA130	Ldi_1	Ac-Res ¼	~ 5

*from AlQahtani et al. (2010)

Teeth from the same archaeological layer

Specimens PA92, PA93 and PA94 were recovered within the same archaeological layer (20d) and could have belonged to the same individual. Unfortunately, their roots are damaged so it has not been possible to precisely determine the root resorption stage (AlQahtani et al., 2010). However, their Sr isotope ratios are equal if we consider the entire observed variability, suggesting that they could possibly belong to the same individual.

Similarly, PA111 and PA112 have been sampled from the same archaeological layer. These two teeth present a comparable root resorption (Rc-A ½) and thus, potentially, they could have belonged to the same individual. PA111 shows a slightly higher Sr isotope ratio (0.70845 ± 0.00027) compared to PA112 (0.70812 ± 0.00053), but still very similar considering the observed intra-tooth variability. Both are within the observed Sr local baseline.

References

AlQahtani SJ, Hector MP, Liversidge HM (2010) Brief communication: the London atlas of human tooth development and eruption. Am J Phys Anthropol 142:481-490.

Ambrose SH (1990) Preparation and characterization of bone and tooth collagen for isotopic analysis. J Archaeol Sci 17:431–451.

Balter V, Braga J, Télouk P, Thackeray JF (2012) Evidence for dietary change but not landscape use in South African early hominins. Nature 489:558–560.

Bentley RA (2006) Strontium isotopes from the earth to the archaeological skeleton: A review. Journal of Archaeological Method and Theory 13:135–187.

Berto C, Boscato P, Boschin F, Luzi E, Ronchitelli A (2017) Paleoenvironmental and paleoclimatic context during the Upper Palaeolithic (late Upper Pleistocene) in the Italian Peninsula. The small mammal record from Grotta Paglicci (Rignano Garganico, Foggia, Southern Italy). Quat Sci Rev 168:30–41.

Binford LR (2001) Constructing frames of reference: An analytical method for archaeological theory building using ethnographic and environmental data sets. University of California Press, Los Angeles.

Bocherens H, et al. (1991) Isotopic biogeochemistry (13C, 15N) of fossil vertebrate collagen: implications for the study of fossil food web including Neandertal Man. J Hum Evol 20:481–492.

Bocherens H, Drucker DG, Germonpré M, Lázničková-Galetová M, Naito YI, Wissing C, Brůžek J, Oliva M (2015) Reconstruction of the Gravettian food-web at Předmostí I using multi-isotopic tracking (13C, 15N, 34S) of bone collagen. Quat Int 359-360:211-228.

Brown TA, Nelson DE, Vogel JS, Southon JR (1988) Improved collagen extraction by modified Longin method. Radiocarbon 30:171–177.

Brock F, Ramsey CB, Higham T (2007) Quality Assurance of Ultrafiltered Bone Dating. Radiocarbon 49:187–192.

Clapperton BK (2006) A review of the current knowledge of rodent behaviour in relation to control devices. Sci Conserv (263):1–55.

Copeland SR, Sponheimer M, Roux PJ, Grimes V, Lee-Thorp JA, Ruiter DJ De, Richards MP (2008) Strontium isotope ratios (87Sr/86Sr) of tooth enamel: a comparison of solution and laser ablation multicollector inductively coupled plasma mass spectrometry methods. Rapid Communications in Mass Spectrometry 22:3187–3194.

Copeland SR, Sponheimer M, de Ruiter DJ, Lee-Thorp JA, Codron D, le Roux PJ, Grimes V, Richards MP (2011) Strontium isotope evidence for landscape use by early hominins. Nature 474:76-78.

Evans JA, Chenery CA, Fitzpatrick AP (2006) Bronze Age childhood migration of individuals near Stonehenge, revealed by strontium and oxygen isotope tooth enamel analysis. Archaeometry 48:309–321.

Herwartz D, Tütken T, Jochum KP, Sander PM (2013) Rare earth element systematics of fossil bone revealed by LA-ICPMS analysis. Geochimica et Cosmochimica Acta. 103: 161-183.

Iacumin P, Bocherens H, Huertas AD, Mariotti A, Longinelli A (1997) A stable isotope study of fossil mammal remains from the Paglicci cave, Southern Italy: N and C as palaeoenvironmental indicators. Earth Planet Sci Lett 148:349-357.

Jacques L, Ogle N, Moussa I, Kalin R, Vignaud P, Brunet M, Bocherens H (2008) Implications of diagenesis for the isotopic analysis of Upper Miocene large mammalian herbivore tooth enamel from Chad. Palaeogeography, Palaeoclimatology, Palaeoecology 266:200-210.

Janssen M, Hill K (2016) An agent-based model of resource distribution on hunter-gatherer foraging strategies: clumped habitats favor lower mobility, but result in higher foraging returns. Simulating Prehistoric and Ancient Worlds, eds. Barceló J, Del Castillo F (Computational Social Sciences, Springer, Cham), pp 159-174.

Lee-Thorp J, Sponheimer M (2003) Three case studies used to reassess the reliability of fossil bone and enamel isotope signals for paleodietary studies. Journal of Anthropological Archaeology 22:208–216.

Longin R (1971) New Method of Collagen Extraction for Radiocarbon Dating. Nature 230:241–242.

Lugli F, Cipriani A, Arnaud J, Arzarello M, Peretto C, Benazzi S (2017a) Suspected limited mobility of a Middle Pleistocene woman from Southern Italy: strontium isotopes of a human deciduous tooth. Sci Rep 7:8615.

Lugli F, Cipriani A, Peretto C, Mazzucchelli M, Brunelli D (2017b) In situ high spatial resolution 87Sr/86Sr ratio determination of two Middle Pleistocene (ca 580 ka) Stephanorhinus hundsheimensis teeth by LA–MC–ICP–MS. Int J Mass Spectrom 412:38–48.

Mannino MA, Richards MP (2018) The role of aquatic resources in 'Italian' hunter-gatherer subsistence and diets. Palaeolithic Italy: Advanced studies on early human adaptations in the Apennine peninsula, eds. Borgia V, Cristiani E (Sidestone Press, Leiden), pp 397-426.

Michel, V., Ildefonse, P., Morin, G. (1995) Chemical and structural changes in Cervus elaphus tooth enamels during fossilization (Lazaret cave): a combined IR and XRD Rietveld analysis. Applied Geochemistry 10: 145-159.

Montgomery J, Evans JA, Horstwood MS (2010) Evidence for long-term averaging of strontium in bovine enamel using TIMS and LA-MC-ICP-MS strontium isotope intra-molar profiles. Environ Archaeol 15:32–42.

Pellegrini M, et al. (2008) Faunal migration in late-glacial central Italy: implications for human resource exploitation. Rapid Commun Mass Spectrom 22:1714–1726.

Pettitt PB, Richards M, Maggi R, Formicola V (2003) The Gravettian burial known as the Prince ("Il Principe"): new evidence for his age and diet. Antiquity 77:15-19.

Richards MP, Pettitt PB, Stiner MC, Trinkaus E (2001) Stable isotope evidence for increase dietary breadth in the European mid-Upper Paleolithic. Proc Natl Acad Sci USA 98:6528-6532.

Richards MP, Harvati K, Grimes V, Smith C, Smith T, Hublin JJ, Karkanas P, Panagopoulou E (2008) Strontium isotope evidence of Neanderthal mobility at the site of Lakonis, Greece using laser-ablation PIMMS. Journal of Archaeological Science 35:1251–1256.

Richards MP (2009) Stable isotope evidence for European Upper Paleolithic human diets. The Evolution of Hominin Diets: Integrating Approaches to the Study of Palaeolithic Subsistence, eds. Hublin, J-J, Richards MP (Springer, Netherlands), pp 251-257.

Ronchitelli A, Mugnaini S, Arrighi S, Atrei A, Capecchi G, Giamello M, Longo L, Marchettini N, Viti C, Moroni A (2015). When technology joins symbolic behaviour: The Gravettian burials at Grotta Paglicci (Rignano Garganico–Foggia–Southern Italy). Quaternary International 359:423-441.

Slovak NM, Paytan A (2011) Applications of Sr Isotopes in Archaeology. In: Baskaran, M. (Ed.), Handbook of Environmental Isotope Geochemistry. Springer, pp. 743–768.

Sponheimer M, Lee-Thorp JA (2006) Enamel diagenesis at South African Australopith sites: Implications for paleoecological reconstruction with trace elements. Geochimica et Cosmochimica Acta 70:1644-1654.

Tafuri MA, Fullagar PD, O'Connell TC, Belcastro MG, Iacumin P, Conati Barbaro C, Sanseverino R, Robb J (2016) Life and Death in Neolithic Southeastern Italy: The Strontium Isotopic Evidence. International Journal of Osteoarchaeology 26:1045-1057.

Talamo S, Richards MA (2011) Comparison of Bone Pretreatment Methods for AMS Dating of Samples >30,000 BP. Radiocarbon 53:443–449.

Trueman CN, Tuross N (2002) Trace elements in recent and fossil bone apatite. Reviews in mineralogy and geochemistry 48:489-521.

Tütken T, Vennemann TW, Pfretzschner HU (2011) Nd and Sr isotope compositions in modern and fossil bones - Proxies for vertebrate provenance and taphonomy. Geochimica et Cosmochimica Acta 75:5951–5970.

Van Klinken GJ (1999) Bone collagen quality indicators for palaeodietary and radiocarbon measurements. J Archaeol Sci 26:687–695.

Willmes M, Kinsley L, Moncel MH, Armstrong RA, Aubert M, Eggins S, Grün R (2016) Improvement of laser ablation in situ micro-analysis to identify diagenetic alteration and measure strontium isotope ratios in fossil human teeth. Journal of Archaeological Science 70:102–116.

Wright LE (2005) Identifying immigrants to Tikal, Guatemala: Defining local variability in strontium isotope ratios of human tooth enamel. Journal of Archaeological Science 32, 555–566.